

*Climate of the Past Discussions* is the access reviewed discussion forum of *Climate of the Past*

# Simulation of the last glacial cycle with a coupled climate ice-sheet model of intermediate complexity

A. Ganopolski<sup>1</sup>, R. Calov<sup>1</sup>, and M. Claussen<sup>2,3</sup>

<sup>1</sup>Potsdam Institute for Climate Impact Research, Potsdam, Germany

<sup>2</sup>Max Planck Institute for Meteorology, Hamburg, Germany

<sup>3</sup>KlimaCampus University Hamburg, Hamburg, Germany

Received: 9 September 2009 – Accepted: 17 September 2009 – Published: 12 October 2009

Correspondence to: A. Ganopolski (andrey@pik-potsdam.de)

Published by Copernicus Publications on behalf of the European Geosciences Union.

CPD

5, 2269–2309, 2009

## Simulation of the last glacial cycle

A. Ganopolski et al.

Title Page

Abstract

Introduction

Conclusions

References

Tables

Figures

◀

▶

◀

▶

Back

Close

Full Screen / Esc

Printer-friendly Version

Interactive Discussion



## Abstract

A new version of the Earth system model of intermediate complexity, CLIMBER-2, which includes the three-dimensional polythermal ice-sheet model SICOPOLIS, is used to simulate the last glacial cycle forced by variations of the Earth's orbital parameters and atmospheric concentration of major greenhouse gases. The climate and ice-sheet components of the model are coupled bi-directionally through a physically based surface energy and mass-balance interface. The model accounts for the time-dependent effect of aeolian dust on planetary and snow albedo. The model successfully simulates the temporal and spatial dynamics of the major Northern Hemisphere (NH) ice sheets, including rapid glacial inception, strong asymmetry between the ice-sheet growth phase and glacial termination. Spatial extent and elevation of the ice sheets during the last glacial maximum agree reasonably well with palaeoclimate reconstructions. A suite of sensitivity experiments demonstrates that simulated ice-sheet evolution during the last glacial cycle is very sensitive to some parameters of the surface energy and mass-balance interface and dust module. The possibility of a considerable acceleration of the climate ice-sheet model is discussed.

## 1 Introduction

Simulation and understanding of glacial cycles, which dominated climate variability over the past several million years, still remain a major scientific challenge. Although a large body of palaeoclimate evidences supports the hypothesis of the Earth's orbital variations as pacemaker for glacial cycles, a number of scientific questions remain unsolved. Among them is the nature of the dominant 100 kyr cyclicity over the past 1 million years, which is not present in the frequency spectrum of the "Milankovitch forcing" (summer insolation in the high latitudes of the Northern Hemisphere, NH). Numerous hypotheses addressing the nature of glacial cycles have been proposed in recent decades, but testing of these hypotheses with comprehensive Earth system models

CPD

5, 2269–2309, 2009

## Simulation of the last glacial cycle

A. Ganopolski et al.

Title Page

Abstract

Introduction

Conclusions

References

Tables

Figures

◀

▶

◀

▶

Back

Close

Full Screen / Esc

Printer-friendly Version

Interactive Discussion



---

**Simulation of the last glacial cycle**A. Ganopolski et al.

---

[Title Page](#)[Abstract](#)[Introduction](#)[Conclusions](#)[References](#)[Tables](#)[Figures](#)[◀](#)[▶](#)[◀](#)[▶](#)[Back](#)[Close](#)[Full Screen / Esc](#)[Printer-friendly Version](#)[Interactive Discussion](#)

represents a challenge due to very long orbital time scales. So-called state-of-the-art comprehensive coupled models of the general circulation of the atmosphere and the ocean (GCMs) are still computationally too expensive to simulate even a single glacial cycle. Until recently simulations of glacial cycles were only possible with rather simple climate-cryosphere models. Such as zonally averaged or two-dimensional energy-balance climate models coupled to simplified ice-sheet models (Pollard, 1982; Deblonde et al., 1992; Gallée et al., 1991). These experiments demonstrated that, when forced by variations of the Earth's orbital parameters, simulated ice sheets experience large variations on all major orbital frequencies (of precessional angle, obliquity and eccentricity) with a clearly asymmetric temporal dynamics consistent with palaeoclimate data. It was also shown by Berger et al. (1999) that glacial-interglacial variations in CO<sub>2</sub> concentration alone cannot drive the glacial cycles. Only when added to the orbital forcing, they considerably improve agreement between simulated and reconstructed glacial cycles. This suggests that climate-carbon cycle feedback plays an important role in shaping glacial cycles. Apart from simplified coupled climate-cryosphere models, a number of simulations of glacial cycles were performed using three-dimensional ice-sheet models forced by patterns of glacial climate changes (e.g. Zweck and Huybrechts, 2003; Charbit et al., 2007) or individual climate forcing components (Abe-Ouchi et al., 2007) obtained separately from the GCMs experiments and scaled usage of palaeoclimate data or output of the ice-sheet models.

In recent years, a new class of models, the so-called Earth system model of intermediate complexity (EMICs; Claussen et al., 2002) became available for the study of glacial cycles. These models are far less computationally demanding than coupled GCMs but incorporate substantial more physical processes than simple models. In particular, several EMICs simulate the most recent glacial inception (around 120–115 kyr BP) in a reasonable agreement with palaeodata, at least, in respect of the total ice volume (Wang and Mysak, 2002; Calov et al., 2005). Stability analysis of the climate-cryosphere system performed in Calov and Ganopolski (2005) has shown that the glacial inception represents a bifurcation transition in the climate-cryosphere

system and that the climate system possesses multiple equilibria within a range of Milankovitch forcing, thus supporting the nonlinear paradigm proposed by Paillard (1998, 2001). Recently, the whole last glacial cycle was simulated with the same climate model, as used in this study, but using a different coupling technique and coupling to another ice sheet model (Bonelli et al., 2009).

The purpose of our paper is to present the results of our simulations of the last glacial cycle with the CLIMBER-2 model, where the climate and ice-sheet components are coupled bi-directionally using a physically based surface energy and mass-balance interface. This work represents a continuation of our previous work (Calov et al., 2005) but with an improved version of the model. It is important to note that in this work, similar to previous modelling studies, we prescribed time-dependent radiative forcing of the major greenhouse gases in addition to orbital forcing. Such type of modelling experiments represent an important test for the climate-cryosphere model but cannot be considered as a decisive test for the Milankovitch theory, since, in the real world, changes in the greenhouse gases concentration are not an external forcing but rather an important internal feedback in the Earth system.

## 2 Model description

The model used for this study is the newest version of CLIMBER-2. It is similar to that described in Calov et al. (2005) (hereafter C05). Since the model and its performance has been described in a number of previous publications, we give here only a short general description and will discuss in more detail only the essential improvements compared to the version used in C05.

The CLIMBER-2 model includes six components of the Earth system: atmosphere, ocean, sea ice, land surface, terrestrial vegetation and ice sheets. The first five components are represented by coarse-resolution modules of intermediate complexity and were described in detail in Petoukhov et al. (2000) and Brovkin et al. (2002). The ice-sheet component is represented by the relatively high-resolution three-dimensional

## Simulation of the last glacial cycle

A. Ganopolski et al.

Title Page

Abstract

Introduction

Conclusions

References

Tables

Figures

◀

▶

◀

▶

Back

Close

Full Screen / Esc

Printer-friendly Version

Interactive Discussion



---

**Simulation of the last glacial cycle**A. Ganopolski et al.

---

[Title Page](#)[Abstract](#)[Introduction](#)[Conclusions](#)[References](#)[Tables](#)[Figures](#)[◀](#)[▶](#)[◀](#)[▶](#)[Back](#)[Close](#)[Full Screen / Esc](#)[Printer-friendly Version](#)[Interactive Discussion](#)

polythermal ice-sheet model SICOPOLIS (Greve, 1997). Unlike the majority of previous studies of glacial cycles, which employed a simple empirical-based parameterisation (the so-called positive degree day approach) for the simulation of the mass balance of the ice sheets, in our model the coupling between climate and ice-sheet components is provided via the high-resolution physically-based Surface Energy and Mass-balance Interface (SEMI) described in C05 (see Fig. 1). Compared to the PDD approach, the physically based SEMI has the important advantage that it is equally applicable to any region of the Earth and to any climate conditions – irrespectively, how different they are from the present one. Moreover, it explicitly accounts for the variations of the shortwave radiation associated with orbital forcing. At last, it directly accounts for the effect of dust deposition on snow albedo. In C05, we have shown that this effect is important for the mass balance of the ice sheets. In the current study, similar to C05, we applied the dust deposition rate based on results of simulations for the present-day and LGM (Last Glacial Maximum) conditions by Mahowald et al. (1999). In addition, we implemented a parameterisation for the dust deposition originating from glacial erosion in the model. This is, according to Mahowald et al. (2006a), an important additional source of dust in the vicinity of the ice sheets. We also explicitly included the direct radiative forcing of the atmospheric dust in the same way as it was done in Schneider et al. (2006). As in C05, the cryosphere component affects climate via changes in surface albedo, elevation and changes in land area caused by sea-level drop. In the present work, we additionally accounted for the freshwater flux into the ocean originating from the ice sheets with explicit coupling of the ice-sheet module to the ocean module. In the following sections, we will describe the most important model improvements compared to the model version used in C05.

## 2.1 Freshwater flux from the ice sheets

Changes in freshwater flux into the ocean caused by growth and decay of the ice sheets primarily affect climate via changes of the Atlantic meridional overturning circulation (AMOC), which is associated with meridional oceanic heat transport and sea ice cover.

---

## Simulation of the last glacial cycle

A. Ganopolski et al.

---

Title Page

Abstract

Introduction

Conclusions

References

Tables

Figures

◀

▶

◀

▶

Back

Close

Full Screen / Esc

Printer-friendly Version

Interactive Discussion



In particular, a reduction of the freshwater into the ocean contributes to a strengthening of the AMOC during rapid growth of the ice sheets, while during episodes of massive ice surges into the ocean (Heinrich events) and glacial terminations an increased fresh-water flux into the ocean leads to a weakening, or even a complete cessation of the AMOC, which considerably affects climate in the North Atlantic realm. Surface melting of ice sheets and iceberg calving into the ocean are simulated by the ice-sheet module. Surface ice-sheet melting was added to the river runoff simulated by the climate component of the model, while calving was treated as surface freshwater flux into the nearest oceanic grid cell. During glacial time, the river routing was differed from the present one and was evolving in time. Hence, in principle, the river routing scheme should be updated regularly taking into account changes in the ice-sheet distribution and land elevation. However, for simplicity we used in this study a constant river routing scheme, that differs from the modern one only in the areas which were covered by the ice sheets in Europe and Northern America. The effect of temporal accumulation of meltwater in periglacial lakes was not taken into consideration and all meltwater from the ice sheets was released into the ocean immediately. Note, that both meltwater and iceberg calving were treated as surface freshwater flux and, hence, the potential effect of penetration of meltwater into the deep ocean with sediment-laden flow was not accounted for.

## 2.2 Radiative forcing of atmospheric dust

Palaeoclimate data indicate that the amount of dust in the atmosphere during glacial times was considerably higher than during interglacials. Modelling studies suggest that enhanced atmospheric dust content during glacial time represented an important additional radiative forcing (e.g. Claquin et al., 2003). This forcing was extremely inhomogeneous spatially and varied seasonally. Recent estimates with GCMs indicate that the global averaged radiative forcing of atmospheric dust during the LGM has the order of magnitude of  $-1 \text{ W/m}^2$ , and according to simulations by Mahowald et al. (2006b) and Schneider et al. (2006) it caused an additional global cooling effect of about 0.5 to

## Simulation of the last glacial cycle

A. Ganopolski et al.

1°C with a stronger cooling in the NH. Note that this is only radiative (shortwave and longwave) forcing of the dust in the atmosphere. The impact of dust on snow albedo was treated separately (see below). Since the simulations of the atmospheric dust radiative forcing are available so far only for the LGM time slice, a parameterisation is needed for the evolution of radiative forcing of the atmospheric dust in the transient experiments. We applied a similar procedure to prescribe the temporal development of the radiative dust forcing as that was used in C05 for the dust deposition rate. Namely, we assume that the additional (compared to the present one) radiative forcing of dust  $R^d$  is proportional to the global ice volume as

$$R^d = R_{\text{LGM}}^d V/V_{\text{LGM}}, \quad (1)$$

where  $R_{\text{LGM}}^d$  is the radiative forcing of dust at LGM aggregated over the coarse climate-module grid cells, the same forcing as was used by Schneider et al. (2005).  $V$  is the simulated NH ice volume and  $V_{\text{LGM}}=100$  m.s.l. (metres of sea-level equivalent) is an approximate estimate for the NH ice volume at the LGM. Obviously, this parameterisation is rather crude. Firstly, the assumption that radiative forcing of dust is directly proportional to the global ice volume is somewhat arbitrary and is not held for any location on Earth. Secondly, the radiative forcing of dust depends not only on the dust loading in the atmosphere but also on surface albedo, which changed considerably during the glacial cycle. These problems can only be avoided by the incorporation of the dust cycle directly into the CLIMBER-2 model; work which is now in progress.

### 2.3 Dust deposition rate

It has been shown already in Warren and Wiscombe (1980) that even a tiny amount of dust (relative concentrations of about 100 parts per million of weight, ppmw) mixed with snow decreases the albedo of fresh snow by 0.1. For old snow, this reduction can even reach 0.3. At their initial growth phase, the major NH ice sheets occurred in areas with rather small dust deposition rates. But during the latter stages of the glacial cycle, the ice sheets spread into areas where dust deposition rates, especially under

Title Page

Abstract

Introduction

Conclusions

References

Tables

Figures

◀

▶

◀

▶

Back

Close

Full Screen / Esc

Printer-friendly Version

Interactive Discussion



---

**Simulation of the last glacial cycle**A. Ganopolski et al.

---

[Title Page](#)[Abstract](#)[Introduction](#)[Conclusions](#)[References](#)[Tables](#)[Figures](#)[◀](#)[▶](#)[◀](#)[▶](#)[Back](#)[Close](#)[Full Screen / Esc](#)[Printer-friendly Version](#)[Interactive Discussion](#)

glacial conditions, became sufficient to appreciably affect the albedo of snow. As it was shown in C05 and confirmed using a more sophisticated model by Krinner et al. (2006), accounting for the effect of dust on snow albedo prevents the growth of the ice sheets in areas with high dust deposition rates, such as Eastern Siberia. Probably even more important, the impact of dust on snow albedo is related to the dust produced due to glacial erosion. According to empirical data (Mahowald et al., 2006a), the dust rate deposition rate associated with this mechanism was as high as 10 to 100 g/m<sup>2</sup>/yr just south of the North American and northern European ice sheets. If a typical annual precipitation of about 500 mm/yr is assumed in these areas, such dust deposition rates would result in average concentration of dust in snow of 20 to 200 ppmw assuming that dust is uniformly mixed with snow over the whole year. In reality, most of the dust associated with glacial erosion is deposited during summer; hence, the concentration of dust in the upper snow layer during snowmelt is expected to be much higher than it would be in case of uniform mixing over the year. Moreover, when snow melts, only a fraction of dust is removed by meltwater and therefore the concentration of dust in snow increases with time. Although the accurate modelling of all these processes is problematic, related uncertainties are not crucial, because a saturation effect occurs for dust concentration in snow of more than 1000 ppmw and the albedo of snow reaches a value comparable with that for dirty ice.

In C05, we implemented a simple technique similar to Eq. (1), which produces a spatial distribution of dust deposition rates at any location using results of present-day and LGM simulations from Mahowald et al. (1999) weighted proportionally to the simulated global ice volume. Such an approach, however, is not justified for the glaciogenic dust, because the sources of glaciogenic dust (and therefore its deposition) are strongly related to the extent of the ice sheets and their internal dynamics. Therefore, it is not justified to apply glaciogenic dust simulated for the LGM ice sheets to other periods with very different configurations of the ice sheets. To resolve this problem, we introduced, in our model, a rather simple parameterisation of dust deposition produced from the glaciogenic sources. This parameterisation is based on the assumption that the emis-

---

**Simulation of the last glacial cycle**A. Ganopolski et al.

---

sion of glaciogenic dust is proportional to the delivery of glacial sediments to the edge of an ice sheet (see Appendix for details). Most of the glaciogenic dust originates from the southern flanks of the ice sheets and this source is significant only for mature ice sheets, which reached well into areas covered by thick terrestrial sediments. Parameters of the glaciogenic dust module were tuned to reproduce the reconstructed rate of dust deposition during the LGM. Simulated glaciogenic dust was added to the dust deposition rate taken from Mahowald et al. (1999). Note that in Mahowald et al. (1999) glaciogenic dust sources were not accounted for.

## 2.4 Sliding parameterisation

As it was shown by modelling studies in Calov et al. (2002) and Calov and Ganopolski (2005), fast sliding processes over areas covered by deformable sediments play an important role in ice-sheet dynamics, both, on millennial and longer time scales. In the current work, we use three types of surfaces underlying the ice sheets: rocks, deformable terrestrial sediments and marine sediments. The first two types correspond to present-day land and were distinguished by prescribing a minimum sediment layer thickness in the data source by Laske and Masters (1997), while all areas which lay below present-day sea level were considered to be covered by marine sediments. Basal sliding appears only if the base of an ice sheet is at the pressure melting point. Only in this case is the sediment type of underlying surface important. Two different sliding laws were applied for rock (Calov and Hutter, 1996) and sediment (C05), while the difference between terrestrial and marine sediment was in the value of the sliding parameter, which is an order of magnitude higher for marine sediment.

## 2.5 Temperature correction for North America

As it was shown in Petoukhov et al. (2000), CLIMBER-2 has a reasonable skill in simulating of spatial and seasonal variability of different climatological fields relevant for ice sheets. In particular, biases in simulated present-day summer temperatures,

[Title Page](#)[Abstract](#)[Introduction](#)[Conclusions](#)[References](#)[Tables](#)[Figures](#)[◀](#)[▶](#)[◀](#)[▶](#)[Back](#)[Close](#)[Full Screen / Esc](#)[Printer-friendly Version](#)[Interactive Discussion](#)

## Simulation of the last glacial cycle

A. Ganopolski et al.

Title Page

Abstract

Introduction

Conclusions

References

Tables

Figures

◀

▶

◀

▶

Back

Close

Full Screen / Esc

Printer-friendly Version

Interactive Discussion



the key climatological factor determining ablation of ice sheets, are within 1–2°C and annual precipitation is typically within 30% of observed values. However, with its coarse spatial grid the CLIMBER-2 model cannot resolve some regional features of climate characteristics which are important for the evolution of ice sheets. This is especially true for North America, which is represented in the model by a single grid column. At the same time, due to orographic and geographic peculiarities, there is a strong zonal temperature gradient over North America, which cannot be resolved by the model but is essential for the development of the Northern America glaciation. Preliminary experiments demonstrated that the lack of this zonal gradient causes a problem for the realistic simulations of the North American ice sheets (see also discussion in Sect. 6). Thereby, we implemented a sub-grid correction for the atmospheric temperature in the North American sector, which has the shape of a dipole and closely resembles the deviations of the observed summer air temperature (corrected for elevation effect) from its zonal mean over North America (Fig. 2). The maximum of this applied temperature correction is 3°C. Although this temperature structure is more representative for the summer season, we kept the temperature correction constant in time, since it is the summer temperature that is most important for the mass balance of an ice sheet. The temperature correction was added to the surface air temperature interpolated from the coarse climate module grid. This temperature correction directly affects the surface sensible heat flux and, in addition, the downward longwave radiation by assuming a linear relationship between temperature and downward longwave radiation.

### 3 Experimental setup

Similar to C05, the model was forced by variations in orbital parameters computed following Berger (1978) and greenhouse gas (GHG) concentrations derived from the Vostok ice core. Unlike C05, we now accounted for two other important GHGs: CH<sub>4</sub> and N<sub>2</sub>O. Since the radiative scheme of the CLIMBER-2 model does not include CH<sub>4</sub> and N<sub>2</sub>O, the radiative effect of these gases was incorporated via the so-called equiv-

## Simulation of the last glacial cycle

A. Ganopolski et al.

Title Page

Abstract

Introduction

Conclusions

References

Tables

Figures

◀

▶

◀

▶

Back

Close

Full Screen / Esc

Printer-friendly Version

Interactive Discussion



alent CO<sub>2</sub> concentration, which is determined as the CO<sub>2</sub> concentration which has the same radiative forcing as the combined radiative forcing of all major greenhouse gases. When computing the equivalent CO<sub>2</sub> concentration, the concentrations of individual greenhouse gases were averaged over thousand years (in case if the resolution of individual records was better than one thousand years). Such averaging reduces millennial scale variability in equivalent CO<sub>2</sub> forcing. When computing equivalent CO<sub>2</sub> concentration, following Hansen et al. (2005), we took into account the fact that the resulting radiative forcing of CH<sub>4</sub> is 40% higher than its pure radiative effect due to methane decomposition in the stratosphere and the production of additional water vapour. In principle, when adding effects of CH<sub>4</sub> and N<sub>2</sub>O to that of carbon dioxide, the equivalent pre-industrial CO<sub>2</sub> concentration is considerably higher than 280 ppm. However, the model was tuned for the pre-industrial  $p(\text{CO}_2)$  value of 280 ppm and to prevent the appearance of warm biases or to avoid the necessity to retune the model parameters, we set the  $p_{eq}(\text{CO}_2)$  for pre-industrial conditions to 280 ppm and calculated the  $p_{eq}(\text{CO}_2)$  in such way to obtained a correct change in radiative forcing of GHGs as compared to the pre-industrial .

All model runs started from the equilibrium state corresponding to the orbital configuration and the concentration of GHGs at 126 kyr BP. The model then was run fully interactively and synchronously for 126 kyr until present-day, thus covering the whole last glacial cycle. Simulated Eemian equilibrium climate is slightly warmer than the present one (Kubatzki et al., 2000) and the Greenland ice sheet is reduced compared to modern. Therefore at the end of the run, the model simulates a larger total ice volume than the initial one.

We will start the discussion of modelling results with the so-called Baseline Experiment (BE). This experiment represents a “suboptimal” subjective tuning of the model parameters to achieve the best agreement between modelling results and palaeoclimate data. Obviously, even with a model of intermediate complexity it is not possible to test all possible combinations of important model parameters which can be considered as free (tunable) parameters. In fact, the BE was selected from about 50 model

---

## Simulation of the last glacial cycle

A. Ganopolski et al.

---

Title Page

Abstract

Introduction

Conclusions

References

Tables

Figures

◀

▶

◀

▶

Back

Close

Full Screen / Esc

Printer-friendly Version

Interactive Discussion



simulations of the last glacial cycle with different combinations of key model parameters. Note, that we consider as “tunable” parameters only parameters of the ice-sheet model and the SEMI interface, while the utilized climate component of CLIMBER-2 is the same as in previous studies, such as those used by C05. In the next section, we will discuss the results of a set of sensitivity experiments, which show that our modelling results are rather sensitive to the choice of the model parameters. Therefore, the simulation of a realistic glacial cycle would represent a too ambitious task if the model was computational too expensive to perform a large set of experiments. The selection of the best fit to the palaeodata is based on several criteria among which are (1) an accurate simulation of the total ice-volume variations over the whole glacial cycle, (2) a correct partition of the total ice volume between individual ice sheets and (3) an agreement between simulated and reconstructed ice sheets during LGM. It is important to note that some systematic biases exist in all model simulations; we were not able to eliminate them with any combination of the model parameters.

## 4 Baseline Experiment

### 4.1 Ice-sheet evolution

Figure 3 shows the BE simulation of the NH ice-volume variations during the last glacial cycle expressed in terms of global sea-level change relative to present-day values in comparison with several palaeoclimate reconstructions. When we compared the model results with sea-level change reconstructions, the problem was that our model does not account for the Southern Hemisphere ice sheets, which, in accordance to different estimates, contributed additional between 10 and 20 m to the LGM sea-level drop. This contribution, estimated by Huybrechts (2002), was added to the modelled NH ice volume and plotted in the figure together with an estimate of the range of sea-level variations based on recent coral data compilations (Lambeck et al., 2002; Thompson and Goldstein, 2006; supplementary data therein) and two independent indirect esti-

## Simulation of the last glacial cycle

A. Ganopolski et al.

Title Page

Abstract

Introduction

Conclusions

References

Tables

Figures

◀

▶

◀

▶

Back

Close

Full Screen / Esc

Printer-friendly Version

Interactive Discussion



mates of the sea-level change based on different methods (Waelbroeck et al., 2002; Siddall et al., 2003). As seen in the figure, the model simulates all major aspect of the ice-volume variations during the whole glacial cycle in reasonable agreement with palaeoclimate estimates. Similarly to C05, initial buildup of the ice sheets during the glacial inception starts soon after 120 kyrBP and already around 110 kyr BP, the ice sheets volume reaches 50 m in sea-level equivalent (m.s.l.). During warm stages 5c and 5a most of the NH ice sheets disappeared, which is the only clear disagreement with the reconstructions. The maximum ice volume (ca. 120 m.s.l.) reached at around 20 kyr BP, i.e. one to several thousand years later than that indicated by palaeoclimate reconstructions. Abrupt deglaciation started soon after 20 kyr BP with the largest rate of the ice-sheet melting of 20 m.s.l. per thousand years (or ca. 0.2 Sv) peaking at around 15 kyr BP, which is in close agreement with observed rate of sea-level rise during the MWP-1A event. The simulated deglaciation of the NH was completed around 7 kyr BP, which is in good agreement with palaeoclimate reconstructions. At the end of the run (i.e. at present time), the remaining ice volume is ca. 4 m.s.l. larger than at the beginning of the experiment, which is primarily attributed to the growth of the Greenland ice sheet and is consistent with the estimates that Eemian sea level was 4–6 m higher than the modern one.

As compared to most previous simulations of the last glacial cycle based on different modelling approaches (e.g. Tarasov and Peltier, 1997; Marshall and Clark, 2002; Zweck and Huybrechts, 2004; Abe-Ouchi, 2007; Charbit et al., 2007; Bonelli et al., 2009), our model simulate much more pronounced (and, in generally, more realistic) variations in the ice volume on the precessional time scale (ca. 20 kyr). This is likely to be explained by fact that the previous modelling studies employed the so-called positive degree day (PDD) approach, which only indirectly accounts for insolation changes. In our model, the mass balance of the ice sheets is computed using a surface energy balance approach, which is more sensitive to variations in insolation.

The area of the NH ice sheets closely follows NH ice volume except for the periods of rapid glacial advances (Fig. 4a, b). For example, during glacial inception the ice-sheet

---

**Simulation of the last glacial cycle**A. Ganopolski et al.

---

[Title Page](#)[Abstract](#)[Introduction](#)[Conclusions](#)[References](#)[Tables](#)[Figures](#)[◀](#)[▶](#)[◀](#)[▶](#)[Back](#)[Close](#)[Full Screen / Esc](#)[Printer-friendly Version](#)[Interactive Discussion](#)

area reaches 1/3 of its maximum (LGM) value already at 115 ky BP, while the total ice volume at that time is only 1/10 of the LGM value. This is explained by an abrupt appearance of large snow fields caused by strong positive snow-albedo feedback as it is discussed in C05. Figure 4c shows the area of the ice-sheet bed which is at pressure melting point (temperate basal area). Not only the absolute area, but also the relative fraction of the temperate basal area has a clear tendency to increase towards the end of the glacial cycle, which is qualitatively similar to results by Marshal and Clark (2002). At the onset of glacial termination, almost one third of the ice-sheet area is temperate at the base, this contributes to rapid deglaciation due to fast sliding of the ice at the southern margins of the ice sheets.

Figure 5 shows the temporal evolution of three major components of the mass balance of the NH ice sheets: accumulation, ablation and ice calving. The total accumulation relatively closely follows the ice-sheet area. Although the area of the NH ice sheets varies by one order of magnitude during the glacial cycle and precipitation decreases considerably during glacial maximum, the averaged precipitation rate over the ice sheets remains surprisingly stable, about 1 mm/day. In turn, ablation and the total mass balance (not shown) of the ice sheets closely follow Milankovitch forcing, even though variations in GHGs also play an important role in shaping the mass balance of the ice sheets. Interesting enough, ablation actually leads Milankovitch forcing by several thousand years, which is explained by the fact that ablation depends also on the area of the ice sheets, which shrinks with increasing insolation. The spikes in the ablation rate during deglaciation are associated with the reorganisation of the thermohaline circulation and the peaks of ice-sheet surface melting approaches 0.3 Sv. Simulated ice sheets calving is rather noisy, which is partly attributed to the numerics of the ice-sheet model. For this reason, the total calving rate shown in Fig. 5 is smoothed by a 10 years running-mean window. Still, it reveals a strong temporal variability; the most pronounced ones are related to the large-scale instability of the Laurentide ice sheet via a mechanism described in Calov et al. (2002) and which resembles in many respects real Heinrich events. During these simulate ice surges the calving rate exceeds

0.1 Sv. Although ablation remains the major negative contribution to the mass balance of the ice sheets over the whole glacial cycle, ice calving plays an important role in the millennial scale variability of AMOC. These simulated abrupt climate shifts resemble real Dansgaard-Oeschger events discussed below.

5 Not only the total NH ice volume, but also the contributions of individual ice sheets agree well with available palaeoclimate reconstructions (Fig. 4). Around LGM, the North American ice sheets contribute with about 70 m to global sea-level drop, while the northern European ice sheets cause approximately 20 m. The glaciation in eastern Siberia, which developed short before the LGM, contributes only a few meters.

10 Figure 6 illustrates extent and elevation of the simulated ice sheets at several time slices. At the maximum of glaciation during MIS4 the ice sheets extended over the area comparable with that during the LGM, but the Laurentide ice sheet was thinner and not connected with the Cordilleran ice sheet (Fig. 6a). Due to higher boreal summer insolation during stage MIS3, both the North American and northern European ice sheets shrunk and, in particular, the ice over Barents Sea disappeared (Fig. 6a, b). It  
15 reappeared only several thousand years before the LGM (Fig. 6b, c). As it was already mentioned above, the glaciation of Alaska and Beringia are too extensive.

At the LGM, the spatial extent of simulated Laurentide ice sheet (Fig. 6c) is close to the ICE-5G reconstruction (Fig. 6d) by Peltier (2004) with a somewhat less southward  
20 penetration of the south-eastern margin of the simulated ice sheet compared to the reconstruction. Compared to ICE-5G reconstruction, the elongated ice dome in the middle of the simulated Laurentide ice sheet is too thin, although our model captures the major topology of this structure. Our model even reproduces a gap in surface elevation between the Laurentide and the Cordilleran ice sheet, which is somewhat  
25 too pronounced in the model. The extent and ice thickness of the Fennoscandian ice sheet, the south-western part of the European ice complex, are in good agreement with the ICE-5G reconstruction, while the north-eastern part of this ice complex does not reach far enough to the east, i.e. there is no ice cover over Kara sea in the simulations, but in the Kara region the reconstructed ice cover is relative small too.

---

## Simulation of the last glacial cycle

A. Ganopolski et al.

---

[Title Page](#)[Abstract](#)[Introduction](#)[Conclusions](#)[References](#)[Tables](#)[Figures](#)[Back](#)[Close](#)[Full Screen / Esc](#)[Printer-friendly Version](#)[Interactive Discussion](#)

---

**Simulation of the last glacial cycle**A. Ganopolski et al.

---

[Title Page](#)[Abstract](#)[Introduction](#)[Conclusions](#)[References](#)[Tables](#)[Figures](#)[◀](#)[▶](#)[◀](#)[▶](#)[Back](#)[Close](#)[Full Screen / Esc](#)[Printer-friendly Version](#)[Interactive Discussion](#)

During termination, the European ice sheets start to contract first in the response to rising summer insolation and GHGs concentration and practically disappeared already at 10 kyr BP. The initial response of the Laurentide ice sheet is slower and only around 15 kyr BP does its retreat accelerates significantly. At around 12 ky BP, the Laurentide and Cordilleran ice sheet separated and the remains of the Laurentide ice sheet on Baffin Island and Labrador completely disappear around 7 kyr BP.

## 4.2 Climate evolution

As it was shown with the CLIMBER-2 model in previous studies (Ganopolski 2003; Schneider et al., 2005), approximately half of the global cooling (compared to present) during the last glacial maximum is explained by presence of the large ice sheets in the NH and the rest by a lowering of the concentrations of the major GHGs (primarily CO<sub>2</sub>), an increase of the atmospheric dust content and shrinking of vegetation cover. Since all these factors are closely related and have a similar temporal dynamics, it is not surprising that the temporal evolution of the globally averaged annual surface air temperature during the glacial cycle follows the same pattern as the ice volume and CO<sub>2</sub>. On regional scale, however, the temperature variations are more complicated and diverse. The northern North Atlantic temperature, which we consider as a proxy for Greenland temperature, apart from strong variations on the orbital time scales, experienced numerous abrupt changes with a magnitude of up to 10°C during a large portion of the glacial cycle (Fig. 7). These tooth-shape fluctuations resemble in many respects Dansgaard-Oeschger events recorded in numerous locations over the NH. Such fluctuations are attributed to rapid reorganisations of the Atlantic Meridional Overturning Circulation (AMOC). The largest perturbation of the AMOC, when circulation almost stalled, coincides with the quasi-regular ice surges from the Laurentide ice sheet discussed in Calov et al. (2002). Other less pronounced variations do not have clearly recognisable causes and results from internal stochastic variations of the freshwater balance of the Northern Atlantic as it was shown in Ganopolski and Rahmstorf (2002). Due to the random nature of millennial-scale variability one cannot expect

one-to-one correspondence between simulated and reconstructed temperatures. For example, the model equivalent of Bølling-Allerød occurs several thousand years early than in reality. However the overall qualitative agreement between model and data is quite instructive.

Antarctic temperature follows more closely the concentration of GHGs, but also is strongly affected by orbital variations (Ganopolski and Roche, 2009). It also has a pronounced millennial scale variability, which is the counterpart of that in the Northern Atlantic and which results from the seesaw mechanism (Crowley, 1992). Similar to Ganopolski and Rahmstorf (2001), the strongest warming events in Antarctica are associated with the largest disturbances of the AMOC caused by the model's equivalent of Heinrich events (Fig. 7).

As discussed above and will be illustrated by simulations below, the dust deposition plays an important role in the simulation of the glacial cycle with our model. As shown in Fig. 8 dust deposition over the NH extra-tropics was significantly higher at the LGM as compared to the interglacial state. While outside of the ice sheets, the dust deposition is prescribed by the weighted mean of modern and LGM dust deposition rates simulated in Mahowald (1999), the glaciogenic sources of dust play the dominant role in the vicinity of the ice sheets (Fig. 8). At the LGM, the simulated values of dust deposition rates just south of both major NH ice complexes exceed  $50 \text{ g}/(\text{m}^2 \text{ yr})$ , which is compatible with empirical data presented in Mahowald et al. (2005). As it is shown in Fig. 8c, the dust deposition rate at the southern edge of the Laurentide ice sheet increases rapidly around LGM and remains high during deglaciation. Simulated amount of dust deposition reduced snow albedo significantly and facilitated the retreat of the ice sheets during deglaciation.

## 5 Sensitivity experiments

The ice-sheet model and the ice sheet-climate interface contain a number of parameters which are not derived from the first principles. They can be considered as “tunable”

### Simulation of the last glacial cycle

A. Ganopolski et al.

Title Page

Abstract

Introduction

Conclusions

References

Tables

Figures

◀

▶

◀

▶

Back

Close

Full Screen / Esc

Printer-friendly Version

Interactive Discussion



parameters. As it was stated above, the BE was subjectively selected from a large suite of experiments as the best fit to empirical data. Below we will discuss results of a number of additional experiments illustrating the sensitivity of simulated glacial cycle to several model parameters. These results show that the model is rather sensitive to a number of poorly constrained parameters and parameterisations what demonstrates the challenges to realistic simulations of glacial cycles with a comprehensive Earth system model.

## 5.1 Sensitivity to the ice-sheet model parameters

The ice-sheet model SICOPOLIS used for our palaeoclimate simulations has two major “free” parameters controlling ice-sheet dynamics. One is the so-called enhancement factor, which appears as a coefficient in the flow law of ice to account for dust impurities in the ice (Paterson, 1994). Therefore, a higher enhancement increases the deformation velocities of the ice. A constant value of 3 for the enhancement factor is often used for the Greenland ice sheet to capture broadly the contribution of dust load deposited of the ice sheet during glacial time and transported deeper in the ice sheet by ice advection. Considering the dust deposition data by Mahowald et al. (1999, 2006) it becomes obvious that the enhancement factor can be much higher for the NH ice sheets, in particular, during glacial times. The other free parameter determines the bottom sliding over the areas where the base of the ice sheet is temperate.

Experiments where the enhancement factor range between 3 and 12 show a rather weak sensitivity of simulated glacial cycles to this parameter (not shown), which is explained by the relatively minor contribution of the deformation velocities, among other factors controlled by the enhancement factor, to the ice-sheet movement (“spreading”) as compared to basal sliding. Another reason for the low sensitivity of the ice dynamics to the enhancement factor lies in the ice-flow temperature coupling: If modelled ice velocities increase due to a higher enhancement factor the ice sheet becomes overall cooler, because colder and less deformable ice is advected downward, which, in turn, counteracts the velocity increase due to the enhancement factor. In contrast, the sen-

## Simulation of the last glacial cycle

A. Ganopolski et al.

Title Page

Abstract

Introduction

Conclusions

References

Tables

Figures

◀

▶

◀

▶

Back

Close

Full Screen / Esc

Printer-friendly Version

Interactive Discussion



sitivity to the parameterisation of sliding processes is rather strong (Fig. 9a). In the experiment where all continental grid points are treated as rocks (ER) and the experiment where all continental grid points were treated as covered by terrestrial sediments (ET) differ considerably. In the first case, even when basal temperature is at pressure melting point, the bottom sliding is rather small and the ice sheets reached at the LGM a much larger thickness than in the BE. In the second case, the ice sheets are much more mobile and considerably thinner than in the BE. Hence, the simulated glacial cycle is rather sensitive to the parameterisation of bottom sliding, a process which is not yet properly understood.

## 5.2 The role of the atmospheric dust

One of the important novelties of the modelling approach used in this study is the explicit treatment of glaciogenic dust. The proposed parameterisation is rather simple and is only weakly constrained by empirical data. To test how sensitive the simulated glacial cycle is to the amount of dust deposition due to glacial erosion, we change empirical parameter  $k_g$  in Eq. (A1) by  $-100\%$ ,  $-50\%$  and  $+100\%$ , i.e. from zero to doubling of the glaciogenic dust deposition rate compared to the Baseline Experiment. As shown in Fig. 9b, the simulated glacial cycle is rather sensitive to the amount of glaciogenic dust deposition, especially during the first part of the cycle and glacial termination. In absence of glaciogenic dust, the simulated ice-sheet volume is large during the whole MIS5 and MIS4. The relative difference decreases during MIS3 and MIS2 due to a number of negative feedbacks, such as the reduction of accumulation under colder climate conditions. During the glacial termination, when the deposition of glaciogenic dust reaches its maximum in BE, the difference becomes large again, and in the absence of glaciogenic dust, almost half of the LGM ice survives the Holocene. In the case of halving and doubling of the standard value of  $k_g$ , the difference with the BE is not so pronounced, which is explained primarily by the logarithmic dependence of snow albedo under low concentration of dust and the saturation effect under very high concentrations. Hence, at least in our model, accounting for the additional source

## Simulation of the last glacial cycle

A. Ganopolski et al.

Title Page

Abstract

Introduction

Conclusions

References

Tables

Figures

◀

▶

◀

▶

Back

Close

Full Screen / Esc

Printer-friendly Version

Interactive Discussion



of dust related to the glacial erosion is crucial for simulating of a complete termination of the glacial cycle although the simulated ice volume is not too sensitive to the uncertainties in the parameterisation of this dust source.

### 5.3 Sensitivity to the parameters of the surface energy and mass-balance interface

The surface energy and mass-balance interface (SEMI) contains a large number of parameters which are not well-defined and (at least within some range) can be considered as “tunable” parameters. Here, we illustrate the sensitivity of modelling results to the so-called refreezing factor, which is the fraction of snow melt that refreezes and hence does not contribute to the net ablation. The refreezing process is rather complicated and its physically-based modelling requires resolving of the diurnal cycle and usage of a multilayer snow-pack model. Neither is feasible so far in the simulations of the global ice-sheet dynamics on time scales of hundred thousand years. That is why we used a constant refreezing parameter in our model. Results of simulations for the range of a refreezing parameter from 0 to 0.4 are shown in Fig. 9c. As one can see, the simulated ice volume is very sensitive to the choice of the refreezing factor.

SEMI includes a number of parameterisations, which are aimed to account for processes which are not explicitly resolved by the coarse-resolution climate component. One such parameterisation is the so-called “slope effect” on precipitation (Eq. (6) in C05). As shown in Fig. 9c, this parameterisation plays an important role. Indeed, in the experiment where this parameterisation was disabled, i.e. precipitation is simply spatially interpolated from the coarse resolution climate grid, the total ice volume is much lower than in the BE. In particular, no ice growth occurs during MIS5b and the LGM ice volume in this experiment is less than half of that in the BE. Clearly, for models like CLIMBER-2, this parameterisation is crucial. However, even modern coupled GCMs used for palaeoclimate studies have too coarse a spatial resolution to resolve this effect properly.

Another attempt to correct unresolved regional climate pattern is the “American tem-

## Simulation of the last glacial cycle

A. Ganopolski et al.

Title Page

Abstract

Introduction

Conclusions

References

Tables

Figures

◀

▶

◀

▶

Back

Close

Full Screen / Esc

Printer-friendly Version

Interactive Discussion



perature dipole” described above. Although, the magnitude of this temperature correction is only 3°C, which is comparable to the typical temperature biases of state-of-the-art climate models, disabling of the temperature correction over North America has a dramatic effect on the simulated glacial cycle (Fig. 9c) comparable to the switching off the slope parameterisation. Interesting enough, disabling of the slope parameterisation and temperature correction have a similar effect on the temporal dynamics of the NH ice volume: in both cases the tooth-shape of 100-kyr cycle essentially disappeared and the ice-volume variability is dominated by obliquity.

## 5.4 Acceleration technique

Simulation of even only one glacial cycle with a state-of-the-art coupled GCM remains computationally extremely demanding. Thereby the possibility of an acceleration of the model runs would be desirable. Since the time scales of the ice sheets are comparable or even longer than periodicity of the orbital forcing, it is not possible to apply any acceleration technique to the ice-sheet model. However, even with a relatively high resolution (ca. 50 km), modern three-dimensional thermomechanical ice-sheet models are computationally inexpensive compared to the climate models. At the same time, the typical time scales of the atmosphere-ocean system is much shorter compared to orbital time scales and, therefore, it would be justified to accelerate the climate component by an artificially stretching the time scales of the external forcing (orbital and GHGs in our case) as it was proposed in Lorenz and Lohmann (2004). In Calov et al. (2009), we have shown that the climate component can be considerably accelerated without significant loss of accuracy in simulation of the glacial inception. Here, we extend this analysis to the whole glacial cycle. Figure 10a shows the simulated global ice volume in three runs with acceleration factors of 5, 10 and 20 in comparison with the (fully synchronous) Baseline Experiment BE. With respect to simulated ice volume, the agreement between accelerated and BE remains reasonably good up to an acceleration factor of 10. The same is true for the globally averaged surface air temperature, although, pronounced millennial scale variability is considerably suppressed already

## Simulation of the last glacial cycle

A. Ganopolski et al.

Title Page

Abstract

Introduction

Conclusions

References

Tables

Figures



Back

Close

Full Screen / Esc

Printer-friendly Version

Interactive Discussion



for a two-fold acceleration. At last, the simulated deep water temperature is affected by acceleration technique (Fig. 10c). Therefore, our experiments indicate that some aspects of the glacial variability on orbital time scales can be successfully reproduced, even when using a large acceleration factor but considerable delay is introduced in the deep ocean evolution. The latter problem can be at least partly mitigated by using in addition of an acceleration scheme for the deep ocean proposed in Liu et al. (2004).

## 6 Discussion and conclusions

We have presented simulations of the last glacial cycle using the Earth system model of intermediate complexity CLIMBER-2, which incorporates the three-dimensional poly-thermal ice-sheet model SICOPOLIS coupled physically-based and fully bi-directionally with the climate component. Compared to our previous work (C05), we additionally introduced radiative forcing of the atmospheric dust and the effect of deposition of dust produced by glacial erosion.

Our experiments demonstrate that the CLIMBER-2 model with an appropriate choice of model parameters simulates rather realistically the major aspects of the last glacial cycle under orbital and greenhouse-gase forcing. In the simulations, the glacial cycle begins with a relatively abrupt lateral expansion of the North American ice sheets and a parallel growth of the smaller northern European ice sheets. During the initial phase of the glacial cycle (MIS5), the ice sheets experience large variations on precessional time scales. Later on, due to decrease of the magnitude of precessional cycle and stabilising effect of low CO<sub>2</sub> concentration, the ice sheets remain large and grow during most of time before reaching its maximum at around 20 kyr BP. The spatial extent of the simulated ice sheets at LGM agrees reasonably well with palaeoclimate reconstructions. Only the eastern part of the European ice complex and Alaska appear to be glaciated too strongly. Simulated components of the mass balance are strongly affected by the ice volume and orbital forcing. Simulated total ablation is closely related to the Milankovitch forcing but leads it by several thousand years, while the total

## Simulation of the last glacial cycle

A. Ganopolski et al.

Title Page

Abstract

Introduction

Conclusions

References

Tables

Figures

◀

▶

◀

▶

Back

Close

Full Screen / Esc

Printer-friendly Version

Interactive Discussion



accumulation closely follows the area covered by the ice sheets.

From about 19 kyr BP, the ice sheets start to retreat with a maximum rate of melting reaching some 0.3 Sv around 15 kyr BP. The northern European ice sheets disappeared first, and the North American ice sheets completely disappeared at around 7 kyr BP. Fast sliding processes and reduction of surface albedo due to deposition of dust play an important role in rapid deglaciation of the NH.

During the second part of the glacial cycle, the Laurentide ice sheet experienced large scale internal oscillations with a typical periodicity of about 7000 years, in many respects resembling observed Heinrich events. During the same period of time, glacial AMOC becomes unstable and experiences numerous transitions between different modes of operation that results in abrupt climate shifts over the North Atlantic realm resembling in magnitude and temporal dynamics observed Dansgaard-Oeschger events. It is important to stress that the model simulates realistic millennial scale climate variability without any explicit external forcing with the same periodicity. Millennial scale climate variability in our model is the results of internal instability of two components of the climate system: ice sheets and AMOC under glacial climate conditions.

Results from a set of sensitivity experiments demonstrate high sensitivity of simulated glacial cycle to the choice of some modelling parameters, and thus indicate the challenge to perform realistic simulation of glacial cycles with the computationally expensive models. At the same time, our results indicate that the computational cost of the simulation of the glacial cycle can be considerably reduced by using of the appropriate acceleration technique. At least as far as the simulated global ice volume is concerned, acceleration with a factor of up to 10 does not disturb significantly the simulation of the glacial cycle.

## Simulation of the last glacial cycle

A. Ganopolski et al.

Title Page

Abstract

Introduction

Conclusions

References

Tables

Figures

◀

▶

◀

▶

Back

Close

Full Screen / Esc

Printer-friendly Version

Interactive Discussion



## Appendix A

### Parameterisation of dust deposition rate

The dust deposition rate in the model is computed as the sum of two components: the “background” dust deposition constituted by the entrainment of dust from bare soil  $D_b$  and the “glaciogenic” dust  $D_g$  originating from the glacial erosion at the periphery of the ice sheets. The first component, as in C05, is computed using results of the time slice simulation by Mahowald et al. (1999) for modern and LGM conditions. The dust deposition rate at each point and time is computed as a weighted sum of modern and LGM dust deposition rates, where the weight coefficient is proportional to the total NH ice volume:

$$D_b = rD_{\text{LGM}} + (1 - r)D_{\text{MOD}},$$

where  $r = V/V_{\text{LGM}}$ ,  $V$  is the NH ice volume (in m.s.l.),  $V_{\text{LGM}} = 100$  m.s.l. is the ice volume at LGM,  $D_{\text{LGM}}$  and  $D_{\text{MOD}}$  are dust deposition rates computed in Mahowald et al. (1999) for LGM and modern conditions respectively.

The deposition of the glaciogenic dust is computed using a rather crude parameterisation based on the assumption that the glaciogenic source of dust is determined by local properties of the ice sheet near its margin and that the lateral transport of dust in the atmosphere can be described by macroturbulent diffusion, namely, the source term for the glacial erosion  $E_g$  was parameterized as

$$E_g = k_g M u_s, \tag{A1}$$

where  $M$  is the annual melting rate of the ice sheet in the marginal grid-cell,  $u_s$  is the sliding velocity of the ice sheet upstream of the considered marginal grid-cell, and  $k_g$  is the only (spatially and temporally independent) free parameter. This parameterisation is only applied to the marginal ice sheet grid cells which have nonzero ice melt and at least has one neighbouring ice free grid cell located on land. If the ice disappeared in a grid cell which previously was a source of glaciogenic dust, the emission rate in

## Simulation of the last glacial cycle

A. Ganopolski et al.

Title Page

Abstract

Introduction

Conclusions

References

Tables

Figures

◀

▶

◀

▶

Back

Close

Full Screen / Esc

Printer-friendly Version

Interactive Discussion



this grid cell decreases exponentially in time with a time scale of decay equal to one thousand years.

Assuming an universal vertical profile of dust in the atmosphere, isotropic macro-turbulent mixing of the aeolian dust with the constant diffusion coefficient  $K$  and the constant residence time of the dust in the atmosphere  $\tau$ , the balance equation for the total dust load in the atmospheric column  $Q$  (in  $\text{g}/\text{m}^2$ ) can be described by the equation

$$E_g + K \Delta Q - \frac{Q}{\tau} = 0, \quad (\text{A2})$$

where  $E_g$  is the emission of glaciogenic dust per unit area,  $\Delta$  is the Laplacian operator and  $\frac{Q}{\tau} = D_g$  is the dust deposition rate. Although Eq. (A2) is simple, solving it on the ice-sheet model grid is computationally expensive. Therefore, we use instead an equivalent but less expensive approach by computing the deposition rate of glaciogenic dust at any location  $(x_0, y_0)$  by integrating the emission of dust due to glacial erosion  $E_g$  over the surrounding area  $\Omega$

$$D_g(x_0, y_0) = \iint_{\Omega} E_g(x, y) f(l) dx dy,$$

where  $l = \sqrt{(x - x_0)^2 + (y - y_0)^2}$  and, due to conservation of mass, the universal function  $f(l)$  from the must satisfy the condition

$$\iint_{\Omega} f(l) dx dy = 1.$$

The function  $f$  was obtained by solving Eq. (A2) numerically for a singular dust source and using  $K = 2 \cdot 10^6 \text{ m}^2/\text{s}$  and  $\tau = 5$  days. The combination of these two parameters gives the length scale  $L = \sqrt{K\tau} = 10^6 \text{ m}$ , which represent the radius of influence of a singular dust source. Since  $f(l)$  decrease rapidly with the distance from the source,

## Simulation of the last glacial cycle

A. Ganopolski et al.

[Title Page](#)[Abstract](#)[Introduction](#)[Conclusions](#)[References](#)[Tables](#)[Figures](#)[◀](#)[▶](#)[◀](#)[▶](#)[Back](#)[Close](#)[Full Screen / Esc](#)[Printer-friendly Version](#)[Interactive Discussion](#)

the size of the integration domain  $\Omega$  can be chosen with sufficient accuracy on the order of magnitude of  $L$ .

Our simulated dust deposition rates due to glacial erosion do not take into account the elevation of the ice sheets, which is unrealistic, since most of dust should be deposited at lower elevations in the vicinity of the ice-sheet margins. However, because dust deposition affects the mass balance of the ice sheets only in the ablation zone, which is typically below 1 km, and the deposition of glacial erosion dust over the ice sheets was not accounted for in the simulation of the surface albedo in the climate component of the model, this overestimation over high-elevated parts of the ice sheets does not affect significantly our modelling results.

*Acknowledgements.* We would like to thank Ralf Greve for providing us with the ice sheet model SICOPOLIS. This project was partly funded by the Deutsche Forschungsgemeinschaft CL 178/4-1 and CL 178/4-2.

## References

- Abe-Ouchi, A., Segawa, T., and Saito, F.: Climatic Conditions for modelling the Northern Hemisphere ice sheets throughout the ice age cycle, *Clim. Past*, 3, 423–438, 2007, <http://www.clim-past.net/3/423/2007/>.
- Berger A.: Long-term variations of daily insolation and Quaternary climatic change, *J. Atmos. Sci.*, 35, 2362–2367, 1978.
- Berger, A., Li, X. S., and Loutre, M. F: Modeling northern hemisphere ice volume over the last 3 million years, *Quaternary Sci. Rev.*, 18, 1–11, 1999.
- Bonelli, S., Charbit, S., Kageyama, M., Woillez, M.-N., Ramstein, G., Dumas, C., and Quiquet, A.: Investigating the evolution of major Northern Hemisphere ice sheets during the last glacial-interglacial cycle, *Clim. Past*, 5, 329–345, 2009, <http://www.clim-past.net/5/329/2009/>.
- Brovkin, V., Bendtsen, J., Claussen, M., Ganopolski, A., Kubatzki, C., Petoukhov, V., and Andreev, A.: Carbon cycle, vegetation and climate dynamics in the Holocene: experiments with the CLIMBER-2 model, *Global Biogeochem. Cy.* 16, 1139, doi:10.1029/2001GB001662, 2002.

## Simulation of the last glacial cycle

A. Ganopolski et al.

Title Page

Abstract

Introduction

Conclusions

References

Tables

Figures



Back

Close

Full Screen / Esc

Printer-friendly Version

Interactive Discussion



**Simulation of the last glacial cycle**

A. Ganopolski et al.

Title Page

Abstract

Introduction

Conclusions

References

Tables

Figures

◀

▶

◀

▶

Back

Close

Full Screen / Esc

Printer-friendly Version

Interactive Discussion



- Calov, R. and Ganopolski, A.: Multistability and hysteresis in the climate-cryosphere system under orbital forcing, *Geophys. Res. Lett.*, 32, L21717, doi:10.1029/2005GL024518, 2005.
- Calov, R., Ganopolski, A., Petoukhov, V., Claussen, M., and Greve, R.: Large-scale instabilities of the Laurentide Ice Sheet simulated in a fully coupled climate-system model, *Geophys. Res. Lett.*, 29, 2216, doi:10.1029/2002GL016078, 2002.
- Calov, R., Ganopolski, A., Claussen, M., Petoukhov, V., and Greve, R.: Transient simulation of the last glacial inception. Part I: Glacial inception as a bifurcation of the climate system, *Clim. Dynam.*, 24, 545–561, doi:10.1007/s00382-005-0007-6, 2005.
- Calov, R., Ganopolski, A., Kubatzki, C., and Claussen, M.: Mechanisms and time scales of glacial inception simulated with an Earth system model of intermediate complexity, *Clim. Past*, 5, 245–258, 2009.
- Calov, R. and Hutter, K.: The thermomechanical response of the Greenland ice sheet to various climate scenarios, *Clim. Dynam.*, 12, 243–260, 1996.
- Charbit, S., Ritz, C., Philippon, G., Peyaud, V., and Kageyama, M.: Numerical reconstructions of the Northern Hemisphere ice sheets through the last glacial-interglacial cycle, *Clim. Past*, 3, 15–37, 2007, <http://www.clim-past.net/3/15/2007/>.
- Claquin, T., Roelandt, C., Kohfeld, K. E., Harrison, S. P., Tegen, I., Prentice, I. C., Balkanski, Y., Bergametti, G., Hansson, M., Mahowald, N., Rodhe, H., and Schulz, M.: Radiative forcing of climate by ice-age atmospheric dust, *Clim. Dynam.*, 20, 193–202, doi:10.1007/s00382-002-0269-1, 2003.
- Claussen, M., Brovkin, V., Calov, R., Ganopolski, A., and Kubatzki, C.: Did humankind prevent a Holocene glaciation? Comment on Ruddiman’s hypothesis of a pre-historic Anthropocene, *Climatic Change*, 69, 409–417, doi:10.1007/s10584-005-7276-2, 2005.
- Claussen, M., Mysak, L. A., Weaver, A. J., Crucifix, M., Fichet, T., Loutre, M.-F., Weber, S. L., Alcamo, J., Alexeev, V. A., Berger, A., Calov, R., Ganopolski, A., Goosse, H., Lohman, G., Lunkeit, F., Mokhov, I. I., Petoukhov, V., Stone, P., and Wang, Z. H.: Earth system models of intermediate complexity: Closing the gap in the spectrum of climate system models, *Clim. Dynam.*, 18, 579–586, 2002.
- Crowley, T. J.: North Atlantic Deep Water cools the southern hemisphere, *Paleoceanography*, 7, 489–497, 1992.
- Deblonde, G., Peltier, W. R., and Hyde, W. T.: Simulations of continental ice sheet growth over the last glacial-interglacial cycle: experiments with a one level seasonal energy balance

---

**Simulation of the last glacial cycle**A. Ganopolski et al.

---

[Title Page](#)[Abstract](#)[Introduction](#)[Conclusions](#)[References](#)[Tables](#)[Figures](#)[◀](#)[▶](#)[◀](#)[▶](#)[Back](#)[Close](#)[Full Screen / Esc](#)[Printer-friendly Version](#)[Interactive Discussion](#)

- model including seasonal ice albedo feedback, *Global Planet. Change*, 6, 37–55, 1992.
- Gallée, H., van Ypersele, J. P., Fichet, T., Tricot, C., and Berger, A.: Simulation of the last glacial cycle by a coupled, sectorially averaged climate-ice sheet model. 1. The climate model, *J. Geophys. Res.*, 96, 13139–13161, 1991.
- 5 Ganopolski, A.: Glacial Integrative modelling, *Philos. T. Roy. Soc. A*, 361, 1871–1884, 2003.
- Ganopolski, A. and Rahmstorf, S.: Rapid changes of glacial climate simulated in a coupled climate model, *Nature*, 409, 153–158, 2001.
- Ganopolski, A. and Rahmstorf, S.: Abrupt glacial climate changes due to stochastic resonance, *Phys. Rev. Lett.*, 88, 038501, doi:10.1103/PhysRevLett.88.038501, 2002.
- 10 Ganopolski, A., Rahmstorf, S., Petoukhov, V., and Claussen, M.: Simulation of modern and glacial climates with a coupled global model of intermediate complexity, *Nature*, 391, 351–356, 1998.
- Ganopolski, A. and Roche, D.: On the nature of leads and lags during glacial-interglacial transitions, *Quaternary Sci. Rev.*, in press, 2009.
- 15 Greve, R.: A continuum-mechanical formulation for shallow polythermal ice sheets, *Philos. T. Roy. Soc. A*, 355, 921–974, 1997.
- Hansen, J., Sato, M., Ruedy, R., Nazarenko, L., Lacis, A., Schmidt, G. A., Russell, G., Aleinov, I., Bauer, M., Bauer, S., Bell, N., Cairns, B., Canuto, V., Chandler, M., Cheng, Y., Del Genio, A., Faluvegi, G., Fleming, E., Friend, A., Hall, T., Jackman, C., Kelley, M., Kiang, N., Koch, D.,
- 20 Lean, J., Lerner, J., Lo, K., Menon, S., Miller, R., Minnis, P., Novakov, T., Oinas, V., Perlwitz, J., Perlwitz, J., Rind, D., Romanou, A., Shindell, D., Stone, P., Sun, S., Tausnev, N., Thresher, D., Wielicki, B., Wong, T., Yao, M., and Zhang, S.: Efficacy of climate forcings, *J. Geophys. Res.*, 110, D18104, doi:10.1029/2005JD005776, 2005.
- Huybrechts, P.: Sea-level changes at the LGM from ice-dynamics reconstructions of the Greenland and Antarctic ice sheets during the glacial cycles, *Quaternary Sci. Rev.*, 21, 203–231, 2002.
- 25 Krinner, G., Boucher, O., and Balkanski, Y.: Ice-free glacial northern Asia due to dust deposition on snow, *Clim. Dynam.*, 27, 613–625, doi:10.1007/s00382-006-0159-z, 2006.
- Kubatzki, C., Montoya, M., Rahmstorf, S., Ganopolski, A., and Claussen, M.: Comparison of the last interglacial climate simulated by a coupled global model of intermediate complexity and an AOGCM, *Clim. Dynam.*, 16, 799–814, 2000.
- 30 Lambeck, K., Esat, T. M., and Potter, E. K.: Links between climate and sea levels for the past three million years, *Nature*, 419, 199–206, 2002.

- Laske, G. and Masters, G. A.: Global Digital Map of Sediment Thickness, EOS Trans., AGU, 78, F483, 1997.
- Liu, Z., Lewis, W., and Ganopolski, A.: An acceleration scheme for the simulation of long term climate evolution, *Clim. Dynam.*, 22, 771–781, 2004.
- 5 Lorenz, S. J. and Lohmann, G.: Acceleration technique for Milankovitch type forcing in a coupled atmosphere-ocean circulation model: method and application for the holocene, *Clim. Dynam.*, 23, 727–743, 2004.
- Mahowald, N., Kohfeld, K. E., Hansson, M., Balkanski, Y., Harrison, S. P., Prentice, I. C., Schulz, M., and Rodhe, H.: Dust sources and deposition during the last glacial maximum and current  
10 climate: A comparison of model results with paleodata from ice cores and marine sediments, *J. Geophys. Res.*, 104, 15895–15916, 1999.
- Mahowald, N., Muhs, D. R., Levis, S., Rasch, P. J., Yoshioka, M., Zender, C. S., and Luo, C.: Change in atmospheric mineral aerosols in response to climate: Last glacial period, preindustrial, modern, and doubled carbon dioxide climates, *J. Geophys. Res.*, 111, D10202, doi:10.1029/2005JD006653, 2006a.
- 15 Mahowald, N., Yoshioka, M., Collins, W. D., Conley, A. J., Fillmore, D. W., and Coleman, D. B.: Climate response and radiative forcing from mineral aerosols during the last glacial maximum, pre-industrial, current and doubled-carbon dioxide climates, *Geophys. Res. Lett.*, 33, L20705, doi:10.1029/2006GL026126, 2006b.
- 20 Marshall, S. J. and Clark, P. U.: Basal temperature evolution of North American ice sheets and implications for the 100 kyr cycle, *Geophys. Res. Lett.*, 29, 2214, doi:10.1029/2002GL015192, 2002.
- Paillard, D.: The timing of Pleistocene glaciations from a simple multiple-state climate model, *Nature*, 391, 378–381, 1998.
- 25 Paillard, D.: Glacial cycles: Toward a new paradigm, *Rev. Geophys.*, 39, 325–346, 2001.
- Paterson, W. S. B.: *The physics of glaciers*, Pergamon/Elsevier, Oxford, 1994.
- Peltier, W. R.: Global glacial isostasy and the surface of the ice-age earth: The ice-5G (VM2) model and grace, *Annu. Rev. Earth Planet. Sci.*, 32, 111–149, 2004.
- Petit, J. R., Jouzel, J., Raynaud, D., Barkov, N. I., Barnola, J. M., Basile, I., Bender, M., Chappellaz, J., Davis, M., Delaygue, G., Delmotte, M., Kotlyakov, V. M., Legrand, M., Lipenkov, V. Y., Lorius, C., Pepin, L., Ritz, C., Saltzman, E., and Stievenard, M.: Climate and atmospheric  
30 history of the past 420000 years from the Vostok ice core, Antarctica, *Nature*, 399, 429–436, 1999.

---

## Simulation of the last glacial cycle

A. Ganopolski et al.

---

[Title Page](#)[Abstract](#)[Introduction](#)[Conclusions](#)[References](#)[Tables](#)[Figures](#)[Back](#)[Close](#)[Full Screen / Esc](#)[Printer-friendly Version](#)[Interactive Discussion](#)

**Simulation of the last glacial cycle**

A. Ganopolski et al.

[Title Page](#)[Abstract](#)[Introduction](#)[Conclusions](#)[References](#)[Tables](#)[Figures](#)[◀](#)[▶](#)[◀](#)[▶](#)[Back](#)[Close](#)[Full Screen / Esc](#)[Printer-friendly Version](#)[Interactive Discussion](#)

- Petoukhov, V., Ganopolski, A., Brovkin, V., Claussen, M., Eliseev, A., Kubatzki, C., and Rahmstorf, S.: CLIMBER-2: A climate system model of intermediate complexity. Part I: Model description and performance for present climate, *Clim. Dynam.*, 16, 1–17, 2000.
- Pollard, D.: A simple ice-sheet model yields realistic 100 kyr glacial cycles, *Nature*, 296, 334–338, 1982.
- Schneider von Deimling, T., Held, H., Ganopolski, A., and Rahmstorf, S.: Climate sensitivity estimated from ensemble simulations of glacial climate, *Clim. Dynam.*, 27, 149–163, doi:10.1007/s00382-006-0126-8, 2006.
- Siddall, M., Rohling, E. J., Almogi-Labin, A., Hemleben, Ch., Meischner, D., Schmelzer, I., and Smeed, D. A.: Sea-level fluctuations during the last glacial cycle, *Nature*, 423, 853–858, doi:10.1038/nature01690, 2003.
- Tarasov, L., Peltier, W. R.: Terminating the 100 kyr ice age cycle, *J. Geophys. Res.*, 102, 21665–21693, 1997.
- Thompson, W. G. and Goldstein, S. L.: A radiometric calibration of the SPECMAP timescale, supplementary data, *Quaternary Sci. Rev.*, 25, 3207–3215, doi:10.1016/j.quascirev.2006.02.007, 2006.
- Waelbroeck, C., Labeyrie, L., Michel, E., Duplessy, J. C., McManus, J. F., Lambeck, K., Balbon, E., and Labracherie, M.: Sea-level and deep water temperature changes derived from benthonic foraminifera isotopic records, *Quaternary Sci. Rev.*, 21, 295–305, 2002.
- Wang, Z. and Mysak, L. A.: Simulation of the last glacial inception and rapid ice sheet growth in the McGill Paleoclimate Model, *Geophys. Res. Lett.*, 29, 2102, doi:10.1029/2002GL015120, 2002.
- Warren, S. G., Wiscombe, W. J.: A model for the spectral albedo of snow. II: snow containing atmospheric aerosol, *J. Atmos. Sci.*, 37, 2734–2745, 1980.
- Zweck, C. and Huybrechts, P.: Modeling the marine extent of Northern Hemisphere ice sheets during the last glacial cycle, *Ann. Glaciol.*, 37, 173–180, 2003.

## Simulation of the last glacial cycle

A. Ganopolski et al.

Title Page

Abstract

Introduction

Conclusions

References

Tables

Figures

◀

▶

◀

▶

Back

Close

Full Screen / Esc

Printer-friendly Version

Interactive Discussion



**Table 1.** Abbreviations of information fluxes shown in Fig. 1.

Abbreviations	Physical meaning
<i>CLD</i>	Total cloud fraction
<i>DDST</i>	Deposition rate of dust
<i>iFRC</i>	Fraction of land covered by ice
<i>iCAL</i>	Ice calving rate into the ocean
<i>iELV</i>	Surface elevation above sea level
<i>iMASK</i>	Ice sheet mask
<i>iMLB</i>	Ice sheet surface mass balance
<i>iMLT</i>	Ice sheet surface melt rate
<i>iSLD</i>	Ice sheet sliding velocity
<i>iTSUR</i>	Ice sheet surface annual temperature
<i>iVOL</i>	Total ice volume
<i>LWR</i>	Downward longwave radiation at the surface
<i>P</i>	Total precipitation rate
<i>RDST</i>	Radiative forcing of aeolian dust
<i>SL</i>	Sea level
<i>SWR</i>	Downward shortwave radiation at the surface
<i>T</i>	Surface air temperature
<i>WND</i>	Module of wind speed

## Simulation of the last glacial cycle

A. Ganopolski et al.

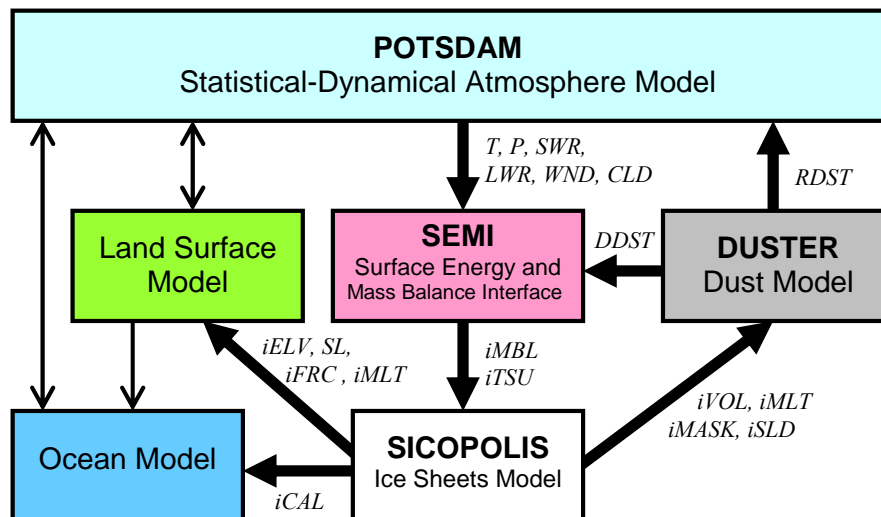


**Fig. 1.** Flow diagram of the model version used in this study. Thick arrows represent new flows of information compared to the “standard” version of CLIMBER-2 described in Petoukhov et al. (2000). Abbreviations are explained in the Table 1.

Title Page

Abstract

Introduction

Conclusions

References

Tables

Figures

◀

▶

◀

▶

Back

Close

Full Screen / Esc

Printer-friendly Version

Interactive Discussion



Simulation of the last  
glacial cycle

A. Ganopolski et al.

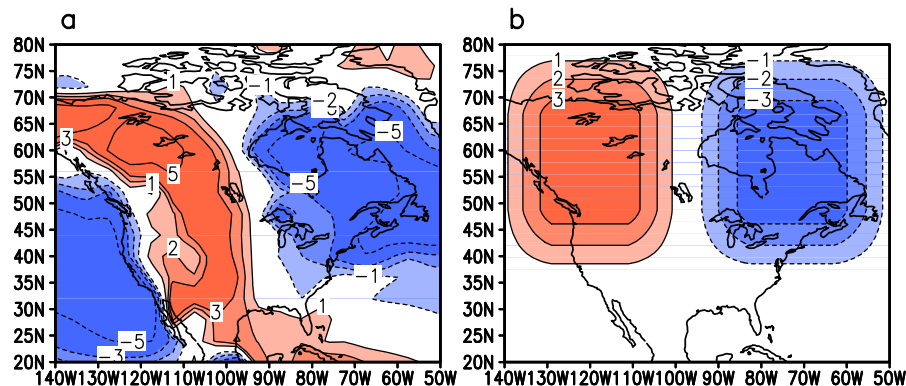


**Fig. 2.** (a) Deviation of observed summer surface air temperature from the zonally averaged over the CLIMBER-2 sector corresponding to North America. (b) Temperature correction added to the interpolated CLIMBER-2 temperature in the SEMI module.

[Title Page](#)[Abstract](#)[Introduction](#)[Conclusions](#)[References](#)[Tables](#)[Figures](#)[◀](#)[▶](#)[◀](#)[▶](#)[Back](#)[Close](#)[Full Screen / Esc](#)[Printer-friendly Version](#)[Interactive Discussion](#)

Simulation of the last  
glacial cycle

A. Ganopolski et al.

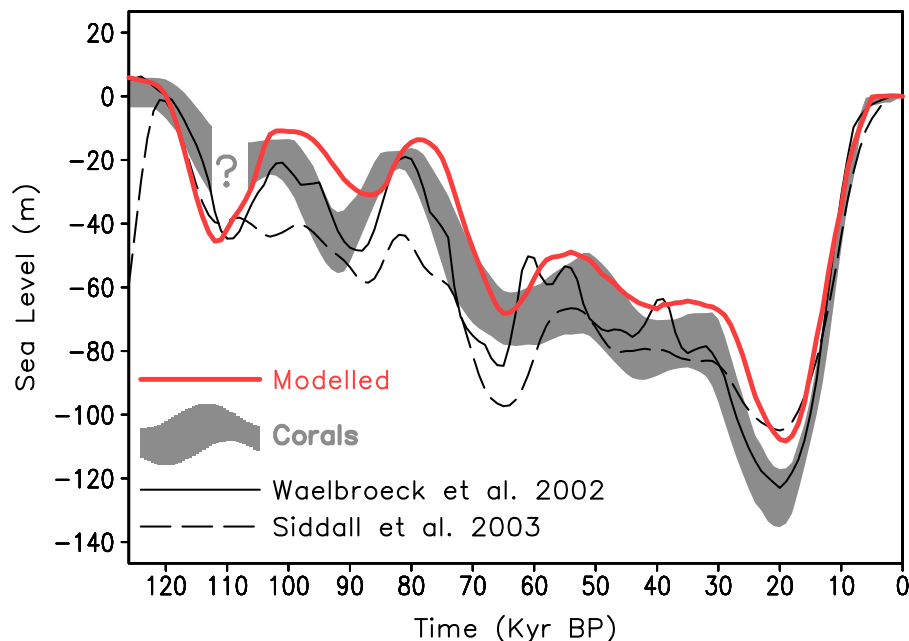


**Fig. 3.** Simulated and reconstructed sea-level evolution during the last glacial cycle relative to present-day values. The red line shows the sum of the simulated Northern Hemisphere (NH) ice volume and the contribution of the Antarctic Ice Sheet (following Huybrechts, 2002) expressed in units of sea level change. The grey area represents an interpretation of recent coral data compilations (Lambeck et al., 2002; Thompson and Goldstein, 2006; supplementary data therein). The width of the interval corresponds to two standard deviations. A very small number of well-dated corals for MIS-5d precludes reliable estimate of the sea level from corals for this period. The solid black line shows the reconstruction by Waelbroeck et al. (2002) based on deep ocean  $^{18}\text{O}$  and temperature records, the dashed black line is the smoothed Siddall et al. (2003) reconstruction based on the Red Sea  $^{18}\text{O}$  record. Smoothing of the data by Siddall is a twofold running average with a 10 kyr window.

[Title Page](#)[Abstract](#)[Introduction](#)[Conclusions](#)[References](#)[Tables](#)[Figures](#)[◀](#)[▶](#)[◀](#)[▶](#)[Back](#)[Close](#)[Full Screen / Esc](#)[Printer-friendly Version](#)[Interactive Discussion](#)

## Simulation of the last glacial cycle

A. Ganopolski et al.

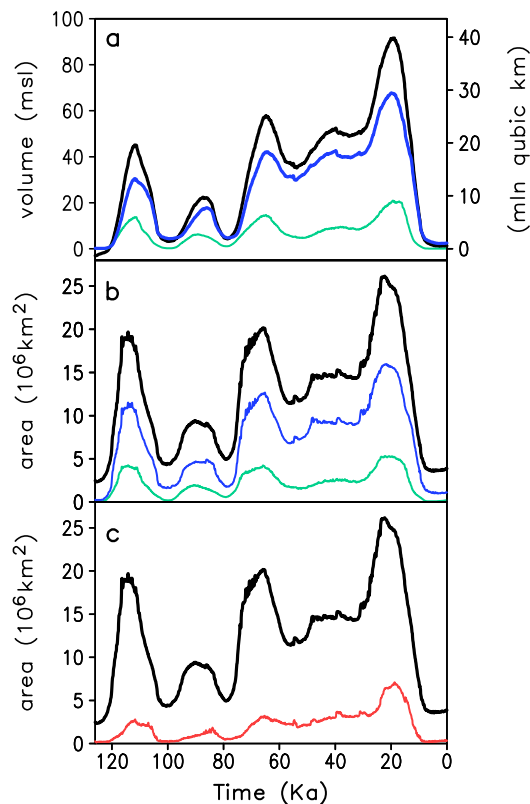


**Fig. 4.** Simulated NH time series. **(a)** ice volume, **(b)** ice area and **(c)** temperate basal area in comparison with the total ice sheets area. The black line shows time series of the entire NH, the blue line of the Northern American and the green line of the European ice sheets. The red line in (c) represents the total NH temperate basal area.

[Title Page](#)[Abstract](#)[Introduction](#)[Conclusions](#)[References](#)[Tables](#)[Figures](#)[◀](#)[▶](#)[◀](#)[▶](#)[Back](#)[Close](#)[Full Screen / Esc](#)[Printer-friendly Version](#)[Interactive Discussion](#)

## Simulation of the last glacial cycle

A. Ganopolski et al.

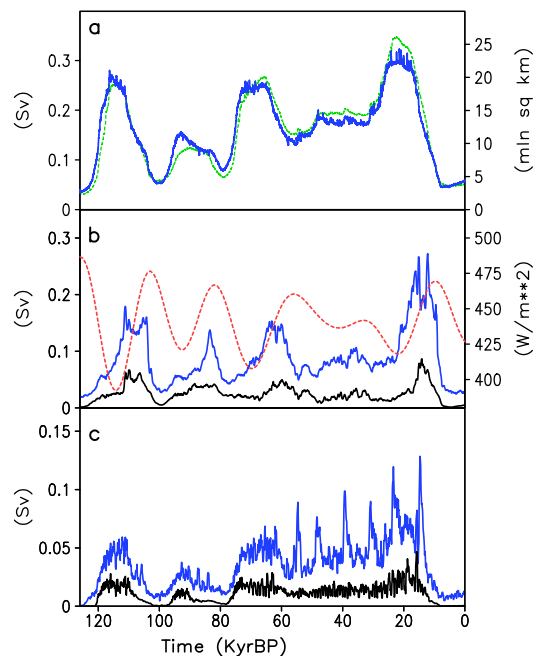


**Fig. 5.** Simulated components of the mass balance of the NH ice sheets. **(a)** Total accumulation (solid blue) and ice-sheet area (dashed green). **(b)** Total surface melting (blue) and surface melt of the European ice sheet (black). Red dashed line show maximum insolation at 65° N. **(c)** Total ice calving (blue) and European ice-sheet calving (black). Units are Sverdrups of water ( $1 \text{ Sv} = 10^6 \text{ m}^3/\text{s}$ ).

Title Page

Abstract

Introduction

Conclusions

References

Tables

Figures

◀

▶

◀

▶

Back

Close

Full Screen / Esc

Printer-friendly Version

Interactive Discussion



Simulation of the last  
glacial cycle

A. Ganopolski et al.

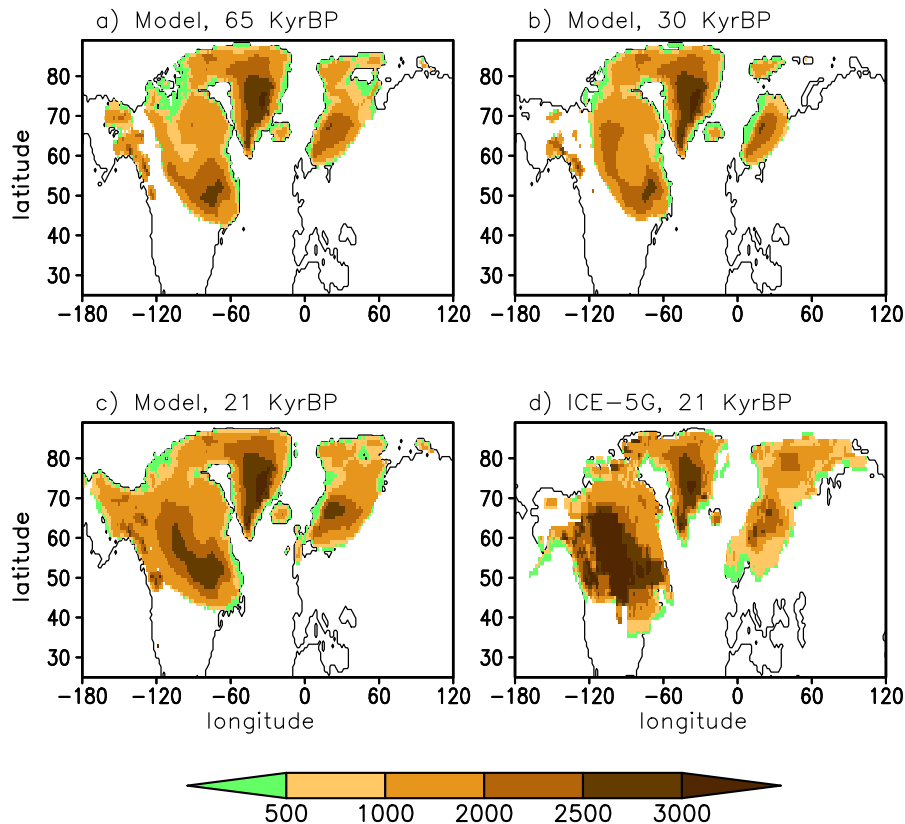


**Fig. 6.** Spatial extent and elevation of simulated (a–c) and reconstructed (d) ice sheets at different time slices. (a) Simulated ice sheets at 65 kyr BP, (b) simulated ice sheets at 30 kyr BP, (c) simulated and (d) reconstructed (Peltier, 2004) ice sheets at the LGM.

[Title Page](#)[Abstract](#)[Introduction](#)[Conclusions](#)[References](#)[Tables](#)[Figures](#)[◀](#)[▶](#)[◀](#)[▶](#)[Back](#)[Close](#)[Full Screen / Esc](#)[Printer-friendly Version](#)[Interactive Discussion](#)

## Simulation of the last glacial cycle

A. Ganopolski et al.

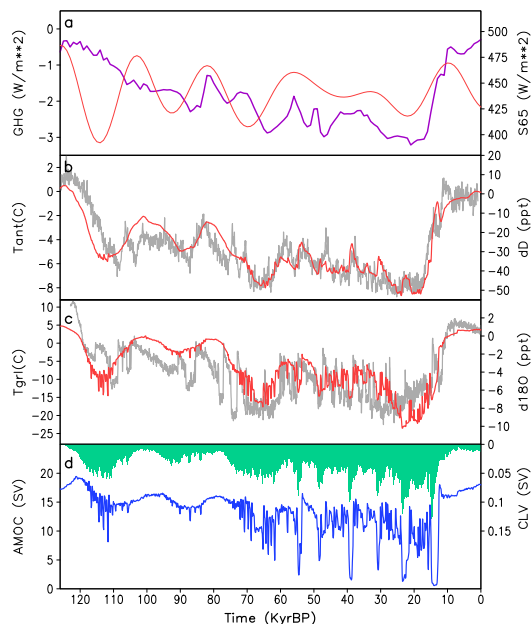


**Fig. 7.** Climate forcing and climate evolution. **(a)** Prescribed radiative forcing of GHGs (dark blue) and orbital forcing (red), here represented by changes in maximum summer insolation at 65° N. **(b)** Simulated annual anomalies of East Antarctic temperature (red) and anomaly of the deuterium concentration from the EPICA ice core (grey). **(c)** Simulated annual anomalies of the North Atlantic (60°–70° N) temperature (red) and measured anomaly of the <sup>18</sup>O concentration from the NGRIP ice core. **(d)** Simulated rate of Atlantic outflow at 30° S (in Sv) and total ice calving (green). Note the reverse direction of y-axis for the calving rate. The anomalies in (b) and (c) are relative to present-day. Although the empirical data are arbitrarily scaled to achieve the best fit with the modelled data, the relationships between temperature variations and isotope variations are close to that used for palaeoclimate reconstructions.

Title Page

Abstract

Introduction

Conclusions

References

Tables

Figures

◀

▶

◀

▶

Back

Close

Full Screen / Esc

Printer-friendly Version

Interactive Discussion



Simulation of the last  
glacial cycle

A. Ganopolski et al.

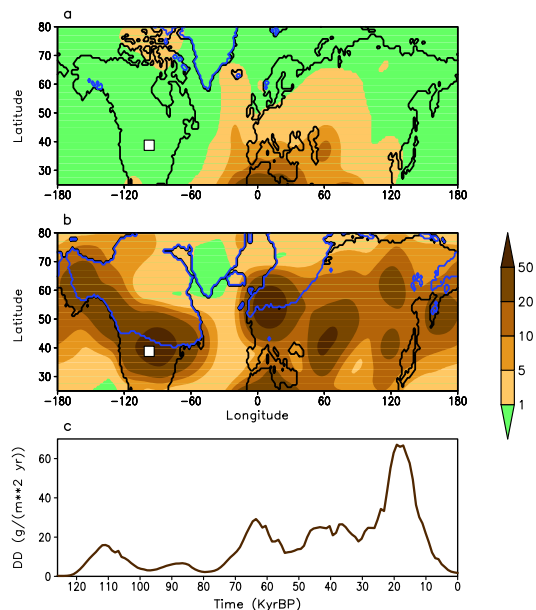


**Fig. 8.** Simulated annual dust deposition rates for **(a)** present-day conditions and **(b)** LGM conditions. **(c)** Simulated evolution of the dust deposition rate (DD) shown in the location south of the Laurentide Ice sheet indicated by the white rectangle in panels (a) and (b). Units are in  $\text{g}/(\text{m}^2 \text{ yr})$ .

[Title Page](#)[Abstract](#)[Introduction](#)[Conclusions](#)[References](#)[Tables](#)[Figures](#)[◀](#)[▶](#)[◀](#)[▶](#)[Back](#)[Close](#)[Full Screen / Esc](#)[Printer-friendly Version](#)[Interactive Discussion](#)

Simulation of the last  
glacial cycle

A. Ganopolski et al.

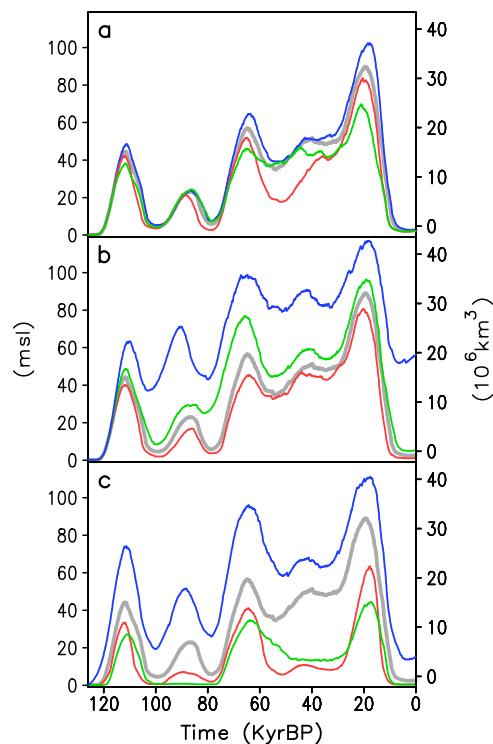


**Fig. 9.** Simulated NH ice volume in a suite of sensitivity experiments. Grey lines in all figures show the Baseline Experiment. **(a)** Sensitivity to sliding parameterisation. The blue line corresponds to the experiment without terrestrial sediments, the red line to the experiment where all land is covered by terrestrial sediments and the green line corresponds to the experiment with the standard sediment mask but enhanced by a factor five sliding parameter. **(b)** Sensitivity to the effect of the glaciogenic dust deposition. The blue line represents the experiment without the effect of dust deposition on snow albedo, the green line with a halved and red line with doubled effect of dust deposition on snow albedo. **(c)** Sensitivity to parameters and parameterisations of the surface energy and mass-balance interface. The blue line indicates the experiment with doubled refreezing fraction of melted snow, the red line represents the experiment without North American temperature dipole correction and the green line stems from the experiment without the slope effect on precipitation rate.

Title Page

Abstract

Introduction

Conclusions

References

Tables

Figures

◀

▶

◀

▶

Back

Close

Full Screen / Esc

Printer-friendly Version

Interactive Discussion



Simulation of the last  
glacial cycle

A. Ganopolski et al.

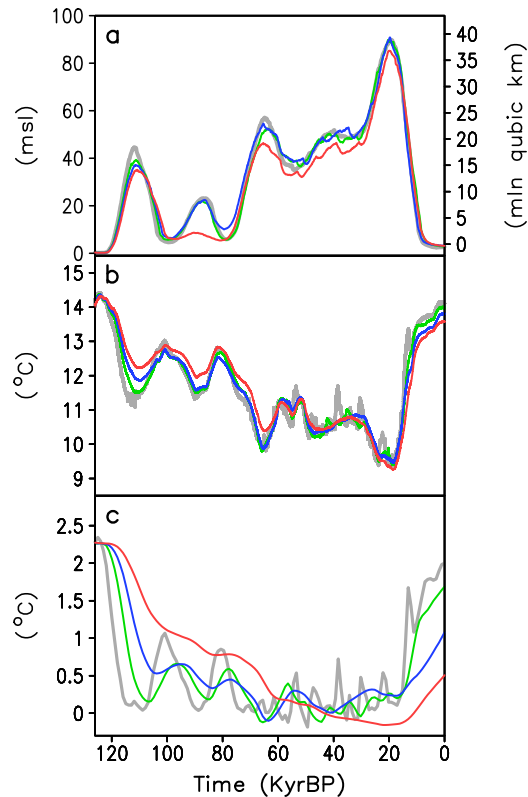


**Fig. 10.** Effect of acceleration of the climate component. **(a)** NH ice volume, **(b)** global annual mean surface air temperature and **(c)** deep Pacific Ocean (4 km) temperature. The grey lines in all figures show the Baseline Experiment. The green, blue and red lines indicate experiments with an acceleration by a factor of 5, 10 and 20, respectively.

[Title Page](#)[Abstract](#)[Introduction](#)[Conclusions](#)[References](#)[Tables](#)[Figures](#)[◀](#)[▶](#)[◀](#)[▶](#)[Back](#)[Close](#)[Full Screen / Esc](#)[Printer-friendly Version](#)[Interactive Discussion](#)